Optical absorption and emission in the defect-chalcopyrite semiconductor $CdGa_2Te_4$

Shunji Ozaki,[a] Kei-Ichi Muto, Hisatoshi Nagata, and Sadao Adachi
Department of Electronic Engineering, Faculty of Engineering, Gunma University, Kiryu-shi, Gunma 376-8515, Japan

(Received 4 October 2004; accepted 9 November 2004; published online 21 January 2005)

Optical-absorption and photoluminescence (PL) spectra have been measured on the defect-chalcopyrite-type semiconductor $CdGa_2Te_4$ in the 0.9–1.5-eV photon-energy range at temperatures between 11 and 300 K. The temperature dependence of the direct-gap energy of $CdGa_2Te_4$ has been determined from the optical-absorption spectra and fit using the Varshni equation and an analytical four-parameter expression developed for the explanation of the band-gap shrinkage effect in semiconductors. The PL spectra show an asymmetric emission band peaking at ~1.326 eV and a symmetric emission band at ~1.175 eV at $T=11$ K, which are attributed to donor-acceptor-pair recombination between exponentially tailed or Gaussian-like donor states and acceptor levels, respectively. A multiple-exponential fit analysis of the PL emission suggests acceptor levels of 50 and 86 meV and a deep donor level of 190 meV, together with an unidentified shallow level of 9 meV. An energy-band scheme has been proposed for the explanation of PL emission observed in $CdGa_2Te_4$. © *2005 American Institute of Physics*. [DOI: 10.1063/1.1845582]

I. INTRODUCTION

The ternary semiconducting compounds $A^{II}B_2^{III}C_4^{VI}$ have been widely investigated because of their potential applications to electro-optic, optoelectronic, and nonlinear optical devices.[1] Most of these compounds have defect-chalcopyrite (space group $=S_4^2$) or defect stannite (space group $=D_{2d}^{11}$) structure.[2] $CdGa_2Te_4$ is one of the defect-chalcopyrite family and is known to have a nearly ideal chalcopyrite structure.[3] Although the material has been the subject of many research efforts, many fundamental properties are not sufficiently evaluated or are even unknown.[4]

Very little is known about the optical properties of $CdGa_2Te_4$.[5,6] Paulavichyus *et al.*[5] performed optical reflection, absorption, and photoconductivity measurements on $CdGa_2Te_4$ films vacuum evaporated on glass substrates. The optical-absorption edge was determined to be ~1.3 eV. Nikolić and Stojilković[6] studied far-infrared reflectivity spectra of bulk $CdGa_2Te_4$ single crystals in the 40–400-cm^{-1} wavenumber range at room temperature. The measured spectra were well characterized by a five harmonic-oscillator model. They reported the high-frequency and static dielectric constants to be $\varepsilon_{\infty\perp}(\varepsilon_{s\perp})=5.73$ (12.04) and $\varepsilon_{\infty\parallel}(\varepsilon_{s\parallel})=6.27$ (11.47), respectively, where $\varepsilon_{\infty\perp}$ ($\varepsilon_{s\perp}$) and $\varepsilon_{\infty\parallel}$ ($\varepsilon_{s\parallel}$) are the high-frequency (static) dielectric constants for light polarized perpendicular and parallel to the tetragonal axis c, respectively.

In our previous paper[7] we synthesized bulk polycrystalline $CdGa_2Te_4$ crystals and measured their ellipsometric and electroreflectance spectra. The measured spectra revealed distinct structures at various critical points, and these structures were assigned to specific points in the Brillouin zone by the aid of a band-structure calculation using empirical pseudopotential method. Room-temperature optical absorption further indicated that $CdGa_2Te_4$ is a direct-band-gap semiconductor having the lowest-direct-gap energy at ~1.36 eV.

In this article we present the optical-absorption and photoluminescence (PL) spectra for $CdGa_2Te_4$ measured at temperatures T between 11 and 300 K. The temperature dependence of the lowest-direct-gap energy E_g for $CdGa_2Te_4$ will be determined from the optical-absorption spectra. The dependence of E_g on T has been commonly described by the empirical equation proposed by Varshni.[8] An analytical expression has been recently proposed by Pässler[9,10] by considering the band-gap shrinkage effect in accordance with general equations and parameter relationships governing the electron-phonon interaction mechanism. The E_g vs T data for $CdGa_2Te_4$ will be analyzed using these two expressions. No PL measurement has been carried out on $CdGa_2Te_4$ to date. We will observe two PL emission bands peaking at ~1.33 and ~1.18 eV at $T=11$ K. These emission bands are attributed to transitions from the exponentially tailed or Gaussian-like donor states and acceptor levels, respectively. The exponentially tailed donor states may be caused by a large number of donors in the defect-chalcopyrite or stannite semiconductors.[1,11]

II. EXPERIMENT

The $CdGa_2Te_4$ crystals used were grown by the conventional Bridgman method reported in the previous paper.[7] They were polycrystalline with grain size of several mm^3. The hot-probe measurements suggested that the electrical conductivity of the samples is p type. The samples were prepared by cutting the ingot with a wire saw, by mechanically polishing, and finally, by chemically etching with a solution of Br_2 in methanol. Thickness of the samples was ~0.1 mm.

[a]Electronic mail: ozaki@el.gunma-u.ac.jp

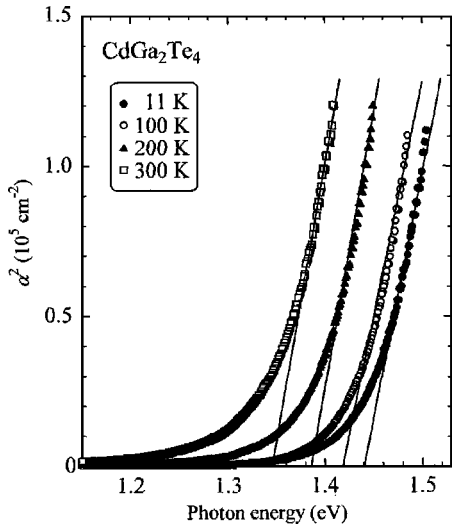

FIG. 1. Plots of the square of the absorption coefficient, α^2, vs photon energy for $CdGa_2Te_4$ at $T=11-300$ K. The intercept point on the energy axis gives the band-gap energy E_g at each temperature.

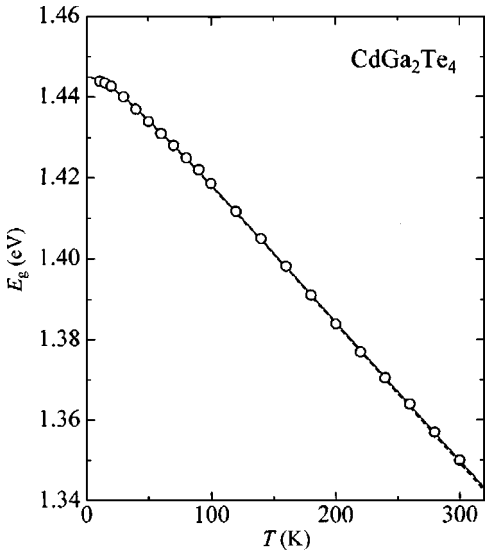

FIG. 2. Plots of E_g vs T for $CdGa_2Te_4$ determined from the optical-absorption measurements. The dashed and solid lines represent the calculated results of Eqs. (3) and (4), respectively. The fit-determined parameters are listed in Table I.

The halogen lamp was used for optical-absorption measurements, and the 488.0-nm line of an Ar^+-ion laser (NEC GLG3110) chopped at 320 Hz was used as the excitation light source for PL measurements. The optical-absorption and PL spectra were taken in the 0.9–1.5-eV photon-energy range using a grating spectrometer (JASCO CT-25C) and a liquid-nitrogen-cooled Ge photodiode (Hamamatsu B6175-05). The spectral resolution of the grating spectrometer used was about ±0.1 nm (±0.2 meV) at the band edge of $CdGa_2Te_4$. The measurements were performed using a closed-cycle refrigerator cryostat (IWATANI CRT105PL) between $T=11$ and 300 K. Note that the experiments were carried out on a few grains of the polycrystalline sample. No attention was, therefore, paid to the polarization dependence of the optical spectra.

III. RESULTS AND DISCUSSION

A. Optical-absorption measurements

One of the most important parameters characterizing semiconducting properties is the band-gap energy E_g. In order to determine the fundamental band-gap energy of $CdGa_2Te_4$, we measured the optical-absorption spectra of the material. The absorption coefficient α was determined from the experimental transmittance T using the relation

$$T=\frac{(1-R)^2e^{-\alpha x}}{1-R^2e^{-2\alpha x}}, \tag{1}$$

where R is the reflectivity. We used a value of $R=0.25$ which was obtained from our previous spectroscopic ellipsometry data.[7]

Figure 1 shows the experimental absorption spectra measured at $T=11-300$ K for $CdGa_2Te_4$. The dependence of α on photon energy E can be written as

$$\alpha(E)=A(E-E_g)^n, \tag{2}$$

where $n=1/2$ and 2 correspond to the direct and indirect band gaps, respectively. We found that the fit is superior for $n=1/2$ than for 2. The fact suggests that $CdGa_2Te_4$ may be a direct-gap semiconductor, in agreement with our band-structure calculation.[7] The plots in Fig. 1 give intercepts, $E_g\sim1.44$ eV ($T=11$ K), ~1.42 eV ($T=100$ K), ~1.38 eV ($T=200$ K), and ~1.35 eV ($T=300$ K), on the energy axis.

Traditionally, temperature variation of the band-gap energy is expressed in terms of Varshni's formula[8]

$$E_g(T)=E_g(0)-\frac{\alpha T^2}{T+\beta}, \tag{3}$$

where $E_g(0)$ is the band-gap energy at $T=0$ K, α is in eV/K, and β is closely related to the Debye temperature of the material (in Kelvin). The dashed line in Fig. 2 represents the least-squares fit of the experimental data to Eq. (3). The fit-determined parameter values are listed in Table I.

Recently, Pässler[9,10] proposed an analytical expression which takes into account the band-gap shrinkage effect in accordance with general equations and parameter relationships governing the electron-phonon interaction mechanism,

$$E_g(T)=E_g(0)-\frac{\alpha_p\Theta_p}{2}\left[\sqrt[p]{1+\left(\frac{2T}{\Theta_p}\right)^p}-1\right], \tag{4}$$

where α_p plays the role of a $T\rightarrow\infty$ limiting value of the band-gap shrinkage coefficient $-\partial E_g(T)/\partial T$, Θ_p is approximately equal to the average phonon temperature, and the power exponent p is closely related to the overall shape of the electron-phonon spectral function in the given material. This expression is more palatable than Eq. (3) from the theoretical point of view. The solid line in Fig. 2 indicates the

TABLE I. Values of $E_g(0)$, α, and β in Eq. (3) and those of α_p, Θ_p, and p in Eq. (4) for $CdGa_2Te_4$.

$E_g(0)$ (eV)	α (meV/K)	β (K)	α_p (meV/K)	Θ_p (K)	p
1.445	0.35	30	0.35	58	1.8

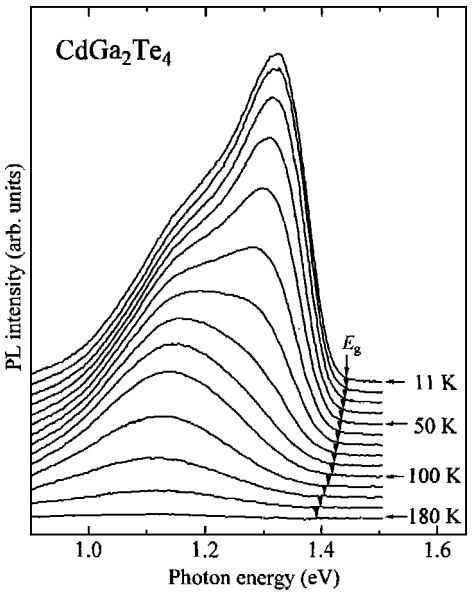

FIG. 3. PL spectra of $CdGa_2Te_4$ measured at $T=11-180$ K. The vertical arrows indicate the positions of the band-gap energy E_g.

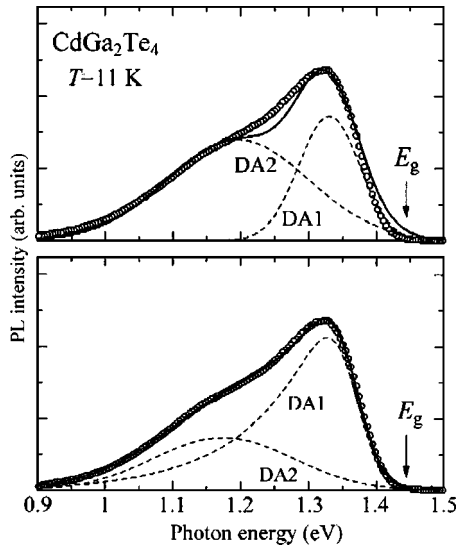

FIG. 4. Theoretical fit of the PL spectrum for $CdGa_2Te_4$ measured at $T=11$ K. The dashed lines in (a) represent the DA-pair components obtained from Eq. (6) (DA1 and DA2), while those in (b) are obtained from Eqs. (10) (DA1) and (6) (DA2). The vertical arrows indicate the position of the band-gap energy E_g at $T=11$ K.

fitted result of the data to Eq. (4). The fit-determined parameters are listed in Table I. We can see in Fig. 2 that these two equations show an equally good agreement with the experimental data in the $T=11-300$-K temperature range.

The effective phonon temperature Θ_p in Eq. (4) is expected to be related to the Debye temperature θ_D by $\Theta_p \sim 2/3\theta_D$.[9] The Θ_p value listed in Table I is 58 K. We can, thus, obtain $\theta_D \sim 87$ K for $CdGa_2Te_4$. No θ_D value has been reported for $CdGa_2Te_4$. We can, however, find that the estimated value of $\theta_D \sim 87$ K is smaller or larger than the CdTe values of $\theta_D \sim 158$ K at $T=0$ K and ~ 44 K at $T=290$ K (Ref. 12), respectively.

Differentiating Eq. (4) with respect to T, we obtain

$$\frac{\partial E_g(T)}{\partial T} = -\alpha_p \left(\frac{2T}{\Theta_p}\right)^{p-1} \left[1 + \left(\frac{2T}{\Theta_p}\right)^{p}\right]^{(1-p)/p}. \tag{5}$$

The temperature coefficient $\partial E_g/\partial T$ for $CdGa_2Te_4$ at $T=300$ K obtained from Eq. (5) is -0.35 meV/K. No $\partial E_g/\partial T$ value has been reported for $CdGa_2Te_4$. However, we can point out that our obtained $\partial E_g/\partial T$ value is in excellent agreement with that for CdTe (-0.36 meV/K).[12]

B. PL measurements

We show in Fig. 3 the PL spectra for $CdGa_2Te_4$ obtained at temperatures between 11 and 180 K. The vertical arrow indicates the position of the band-gap energy E_g at each temperature. It is evident from Fig. 3 that at low temperatures, the PL spectra show the dominant emission peak at ~ 1.3 eV (DA1) with a shoulder at ~ 1.2 eV (DA2). At temperatures higher than ~ 120 K, the ~ 1.3-eV emission peak becomes very weak and, as a result, the low-energy shoulder is observed only as the single emission peak. No band-edge emission has been recognized in the PL spectra even at low temperatures.

The donor-acceptor (DA)-pair emission band can be modeled using a Gaussian line shape as

$$I_{\mathrm{DA}}(E) = S_{\mathrm{DA}} \exp\left[-\frac{(E-E_p)^2}{\Gamma^2}\right], \tag{6}$$

where E_p is the DA-pair emission-peak energy, and S_{DA} and Γ are the strength and spectral width parameters, respectively.

Figure 4(a) shows the fitted result of the experimental PL spectrum measured at $T=11$ K (open circles) to Eq. (6) by taking into account the two Gaussian peaks, DA1 and DA2. It is evident from Fig. 4(a) that the simple Gaussian line-shape model gives no good agreement with the experimental data, especially at both sides of the DA1 emission band (~ 1.33 eV).

In order to achieve a better fit with the experimental data, we assume that the density of states in the conduction-band tail of the DA1 emission band depends exponentially on the energy distance from the unperturbed conduction-band edge[13]

$$N_{D1}(E,T) = \begin{cases} \dfrac{N_{D1}^0}{1 + A_1 e^{-E_{D1}^{\mathrm{eff}}/kT}} \exp[m(E-E_d)], E \leqslant E_d \\ 0, E > E_d, \end{cases} \tag{7}$$

where $E_{\mathrm{D1}}^{\mathrm{eff}}$ is the effective (or "center-of-gravity") energy of the exponentially tailed donor states (see Fig. 9, below), E_d is the so-called "demarcation level" of the donor states, N_{D1}^0 is the density of donor states at $E=E_d$ and $T=0$ K, and m is the slope of the conduction-band tail. Here, the $E_{\mathrm{D1}}^{\mathrm{eff}}$ term is introduced in order to take into account the thermal excitation of the exponential donor electrons into the conduction band (see Fig. 6, below). The slope parameter m is assumed to be independent of T.

The exponentially tailed donor states may arise from the failure in the periodic distribution of the stoichiometric voids in the defect-chalcopyrite structure.[11] Anedda *et al.*[14] mea-

sured the photoconductivity of $CdIn_2S_4$ and found a high density ($\sim 10^{20}$ cm^{-3}) of electron trap levels with an exponential distribution in energy. They explained such higher-density electron traps in terms of higher disorder in the cation sublattice. The same electron traps as in $CdIn_2S_4$ have been observed in $ZnIn_2Se_4$ (Ref. 15) and other isostructural $A^{II}B_2^{III}C_4^{VI}$ semiconductors.[1,11]

The acceptor states are assumed to exhibit a broadened Gaussian distribution given by

$$N_{A1}(E,T) = \frac{N_{A1}^0}{1 + B_1 e^{-E_{A1}/kT}} \exp\left[- \frac{(E - E_{A1})^2}{\Gamma^2} \right], \quad (8)$$

where N_{A1}^0 is the acceptor concentration, E_{A1} is the acceptor ionization energy, and Γ is the width parameter of the acceptor states.

As we will see later, the temperature dependence of the PL intensity for the ~1.33-eV peak (DA1 did not show a simple exponential behavior, $\exp(E_{A1}/kT)$, defined by an activation energy E_{A1} of the acceptor states. We found that the experimental results can be well explained by a double-exponential fit.[16] Note that the photogenerated carrier distribution in localized states cannot be described by thermal equilibrium conditions. We, therefore, modify Eq. (8) by taking into account the double-exponential fit model as[16]

$$N_{A1}(E,T) = \frac{N_{A1}^0}{1 + B_1 e^{-E_{A1}/kT} + C_1 e^{-E_X/kT}} \times \exp\left[- \frac{(E - E_{A1})^2}{\Gamma^2} \right]. \quad (9)$$

Note that the double-exponential fit model promises the presence of another acceptor level at an energy E_X.

The resultant DA-pair recombination intensity $I_{DA1}(E,T)$ can be given by the convolution integral as[13]

$$I_{DA1}(E,T) = P_{DA1} \int N_{A1}(E',T) N_{D1}(E' + E, T) dE', \quad (10)$$

where P_{DA1} is the DA-pair (DA1) transition probability which is assumed to be independent of E and T. The parameters Γ and E_d influence essentially the peak width and asymmetry of the spectrum, respectively. The m value to be fit determined below is 9.2 eV^{-1}.

Figure 4(b) shows the fitted result of the experimental PL spectrum using Eq. (10) for the DA1 emission. The contribution of the DA2 emission is assumed to be given by Eq. (6). Individual contributions of the DA1 and DA2 emission bands are shown in Fig. 4(b) by the dashed lines. Assuming the exponentially tailed donor density of Eq. (7), the theoretical calculation begins to show excellent agreement with the experimental data over the entire photon-energy range. Note that this type of luminescence has been commonly found in spectra of defect-chalcopyrite and stannite $A^{II}B_2^{III}C_4^{VI}$ semiconductors, such as $CdGa_2Se_4$,[17] $CdIn_2Te_4$,[18] $CdIn_2S_4$,[19,20] $ZnGa_2Se_4$,[21] $ZnIn_2S_4$,[13] and $ZnIn_2Te_4$ (Ref. 22) (see also Refs. 1 and 11), although no detailed analysis has been performed up to date.

We show in Fig. 5 the temperature dependence of the DA-pair emission energies, E_p (DA1) and E_p (DA2), and the

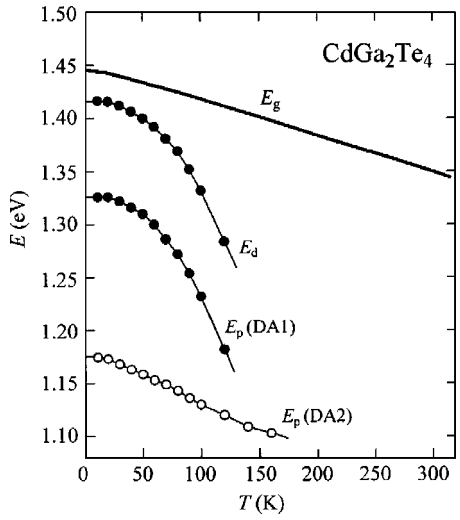

FIG. 5. Variations of the band-gap energy E_g, demarcation level width E_d, and DA-pair peak energies E_p's as a function of temperature T for $CdGa_2Te_4$.

demarcation level width E_d for $CdGa_2Te_4$. For comparison, the temperature dependence of E_g is plotted by the heavy solid line. As similar to E_g, E_p (DA2) decreases with increasing T. E_p (DA1) and E_d, on the other hand, decrease more rapidly than E_g. The temperature coefficients for E_p (DA1) and E_d are found to be about −2.5 meV/K at $T \sim 120$ K, which is an order larger than that for E_g (−0.35 meV/K, see Fig. 2).

The DA-pair emission energy can be theoretically expressed as $E_p(T) = E_g(T) - E_A - E_D + (e^2/4\pi\varepsilon r)$, where r is the paired DA distance. The lowest possible DA-pair energy is given in the limit $r \to \infty$ by $E_p(T) = E_g(T) - E_A - E_D$. The dependence of E_p on T may, thus, be very similar to $E_g(T)$. Besides the band-structure change induced by thermal expansion of the lattice, the temperature dependence of E_g is known to be mainly due to the electron-phonon interaction.

The temperature coefficients for E_p and E_d, −0.2 meV/K at $T \sim 150$ K, observed in $ZnIn_2Te_4$ were about twice smaller than that for E_g (−0.43 meV/K).[22] The very weak temperature dependence of E_p in this material resembles deep-center luminescence typically observed in II-VI semiconductors.[23] A very shallow localized level, for which the electron orbital extends many interatomic spacing, can be reasonably assumed to interact with the host-lattice phonons and the local modes can be neglected. A highly localized deep luminescence center as the self-activated center in II-VI semiconductors, on the other hand, can be interpreted by the configurational coordinate model. It is unclear that the exponential-donor–acceptor-pair states in defect-type semiconductors are highly localized or not; however, it is likely that they interact not only with the fundamental mode of vibration but also with a number of phonon modes. This may lead to the unusual temperature dependence of the DA-pair emissions observed in $CdGa_2Te_4$ (Fig. 5), $ZnIn_2Te_4$ (Ref. 22), and $AgIn_5S_8$ (Ref. 24).

The demarcation level width E_d in $ZnIn_2Te_4$ at $T = 11$ K was found to be ~0.01 eV smaller than E_g.[22] However, its temperature variation was much smaller than that of

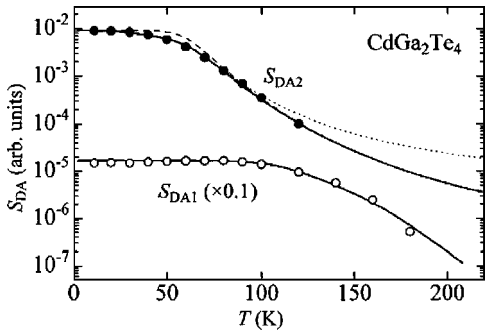

FIG. 6. Variations of the strength parameters S_{DA1} and S_{DA2} as a function of temperature T for $CdGa_2Te_4$. The solid lines show the calculated results of Eqs. (11) (S_{DA1}) and (13) (S_{DA2}), respectively. The dashed and dotted lines are also calculated from Eq. (11) by putting $C_1=0$ (i.e., neglecting E_X) or $A_1=0$ (i.e., neglecting E_{D1}^{eff}), respectively.

E_g and, thus, a crossover occurred between E_g and E_d at $T \sim 90$ K. Then, for $T>90$ K ($E_d>E_g$) a part of the donor electrons in the demarcation levels can be transferred to the conduction band, resulted in an appearance of the band-edge (E_g) emission [see Fig. 8(c) in Ref. 22]. On the other hand, no E_g-E_d crossover can be found in $CdGa_2Te_4$ over $T=11$ and 300 K (Fig. 5). We can, therefore, never observe any band-edge emission in PL of $CdGa_2Te_4$ (see Fig. 3).

The temperature-dependent strength parameter of the DA1 emission can be written from Eqs. (7)–(10) as

$$S_{DA1}(T) = \frac{S_{DA1}^0}{(1+A_1 e^{-E_{D1}^{eff}/kT})(1+B_1 e^{-E_{A1}/kT}+C_1 e^{-E_X/kT})}, \tag{11}$$

with

$$S_{DA1}^0 = N_{D1}^0 N_{A1}^0 P_{DA1}. \tag{12}$$

Similarly, the strength parameter of the DA2 emission can be written as

$$S_{DA2}(T) = \frac{S_{DA2}^0}{(1+A_2 e^{-E_{D2}/kT})(1+B_2 e^{-E_{A2}/kT})}, \tag{13}$$

with

$$S_{DA2}^0 = N_{D2}^0 N_{A2}^0 P_{DA2}. \tag{14}$$

In Fig. 6, we show the variations of S_{DA} for the DA1 and DA2 emission bands as a function of temperature T. The solid lines represent the calculated results of Eqs. (11) and (13) with $S_{DA1}^0=9.12\times10^{-3}$, $A_1=50$, $B_1=7000$, $C_1=3.5$ [Eq. (11)] and $S_{DA2}^0=1.65\times10^{-4}$, $A_2=2\times10^5$, $B_2=2800$ [Eq. (13)], respectively. The activation energies determined here are $E_{A1}=50$ meV, $E_X=9$ meV, and $E_{D1}^{eff}=47$ meV [Eq. (11)]; $E_{A2}=86$ meV and $E_{D2}=190$ meV [Eq. (13)], respectively. The dashed and dotted lines in Fig. 6 are also obtained by putting $C_1=0$ (i.e., neglecting E_X) or $A_1=0$ (i.e., neglecting E_{D1}^{eff}) into Eq. (11), respectively. No good agreement can be achieved between these calculated results and experimental data.

Figure 7 shows the full width at half maximum W for the DA1 and DA2 emission bands as a function of temperature T in $CdGa_2Te_4$. One of the important results of the configurational coordinate model is the form of the temperature dependence of the emission band width $W(T)$ (Ref. 23)

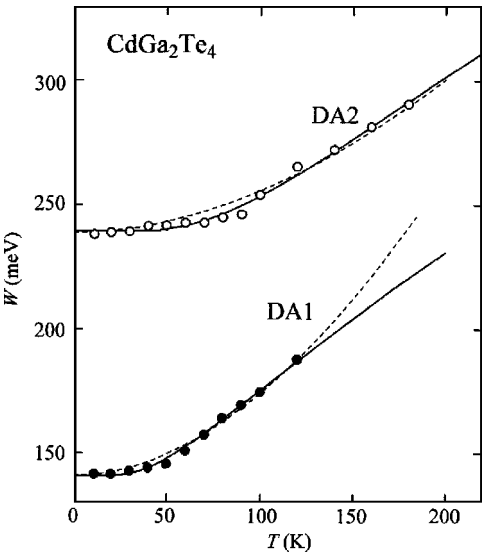

FIG. 7. Variations of the spectral widths W for the DA1 and DA2 emissions as a function of temperature T for $CdGa_2Te_4$. The solid and dashed lines represent the calculated results of Eqs. (15) and (16), respectively. The fit-determined parameters are listed in Table II.

$$W(T) = A + B\left[\coth\left(\frac{\hbar\omega_q}{2kT}\right)\right]^{1/2}, \tag{15}$$

where $\hbar\omega_q$ is the energy of the vibrational mode that interacts strongly with the luminescence center in its exited electronic states. The solid lines in Fig. 7 show the calculated results of Eq. (15). The fitting parameters are given in Table II. We find that the $\hbar\omega_q$ value of 23 meV for the DA2 emission is nearly the same as that of the longitudinal-optical (LO) phonons in CdTe ($\hbar\omega_{LO}\sim21$ meV, Ref. 12), while the $\hbar\omega_q$ value of 13 meV for the DA1 emission is much smaller than the LO-phonon value in CdTe, $\hbar\omega_{LO}\sim21$ meV. It is not clear at present where the smaller $\hbar\omega_q$ value determined for the DA1 emission corresponds to its unique temperature dependence of E_p (see Fig. 5) or not.

The dashed lines in Fig. 7 represent the fitted results using an expression

$$W(T) = W(0) + \frac{\alpha T^2}{T+\beta}, \tag{16}$$

where $W(0)$ is the $T=0$-K value. Note that this expression has the same form as the Varshni's equation of Eq. (3). The $W(0)$, α, and β values determined here are listed in Table II. It is seen in Fig. 7 that Eq. (16) shows a poorer agreement with the experimental data compared with Eq. (15).

TABLE II. Values of A, B, and $\hbar\omega_q$ in Eq. (15) and those of $W(0)$, α, and β in Eq. (16) for $CdGa_2Te_4$.

	A (meV)	B (meV/K)	$\hbar\omega_q$ (meV)	$W(0)$ (meV)	α (meV/K)	β (K)
DA1	7.3	134	13	141	3.6	1000
DA2	35	205	23	239	1.8	1000

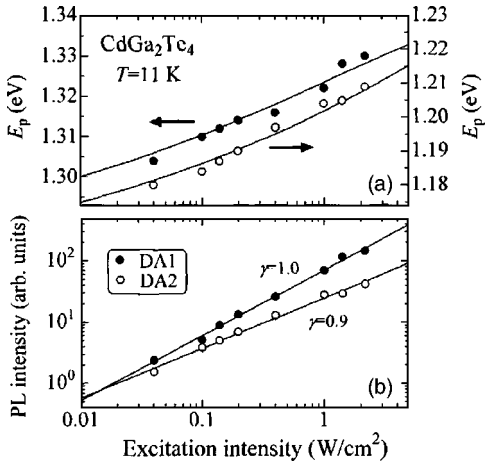

FIG. 8. (a) Excitation intensity dependence of the PL peak energies E_p's and (b) integrated PL intensities for the DA1 and DA2 emissions in $CdGa_2Te_4$ at $T=11$ K. The solid lines in (a) and (b) are calculated from Eqs. (17) and (18), respectively.

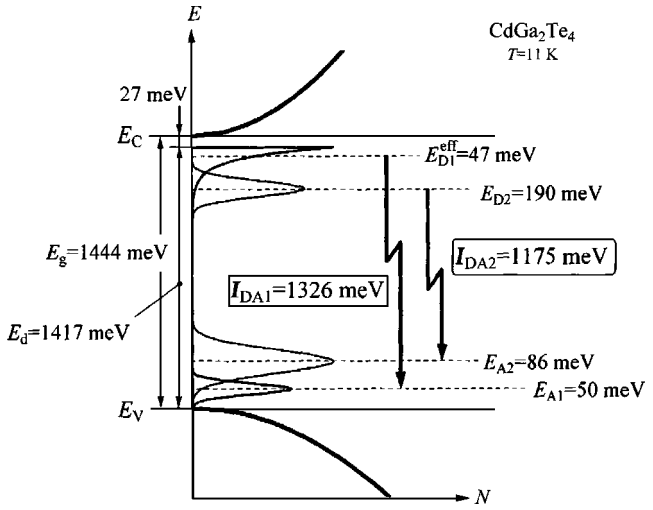

FIG. 9. Proposed energy-band scheme and optical transitions in $CdGa_2Te_4$ at $T=11$ K.

The PL spectra observed in $CdGa_2Te_4$ showed the two DA-pair emission bands; asymmetric DA1 and symmetric DA2 bands. In order to confirm these two bands as actually due to the DA-pair emissions, we examined the excitation intensity dependence of the PL peak energy and integrated emission intensity at $T=11$ K. Figure 8 presents the results of these experiments. It is seen in Fig. 8(a) that the DA1 (DA2) peak energy E_p increases from 1.302 (1.177) to 1.330 eV (1.209 eV) as the laser excitation intensity increases from 0.02 to 2 W/cm^2. For the DA-pair recombination, the excitation laser power I_{ex} can be expressed, as a function of PL peak energy E_p, as[24]

$$I_{ex} = I_0 \frac{(E_p - E_\infty)^3}{(E_B - E_\infty - 2E_p)} \exp\left[- \frac{2(E_B - E_\infty)}{E_p - E_\infty} \right], \tag{17}$$

where I_0 is a proportionality constant, E_B is the emitted photon energy of a close DA pair separated by a shallow-impurity Bohr radius, and E_∞ is the emitted photon energy of an infinity distant DA pair. The solid lines in Fig. 8(a) represent the fitted results of the experimental E_p values to Eq. (17). The fit-determined DA1 (DA2) parameters are $E_B = 1.43$ eV (1.43 eV) and $E_\infty = 1.25$ eV (1.11 eV). We can find that these parameters satisfy the DA-pair emission requirement of $E_\infty \leqslant E_p = 1.302-1.330$ eV ($E_p = 1.177-1.209$ eV) $\leqslant E_B$ for the DA1 (DA2) emission.

The integrated PL intensity I vs I_{ex} can be given by the simple power law[24]

$$I \propto I_{ex}^{\gamma}. \tag{18}$$

The dimensionless exponent γ is known to be $1<\gamma<2$ for free-exciton or bound-exciton emission and $\gamma \leqslant 1$ for free-to-bound or DA-pair emission. The solid lines in Fig. 8(b) represent the fitted results of the experimental data to Eq. (18). The γ values, 1.0 (DA1) and 0.9 (DA2), support the assignment of these PL emissions to DA-pair recombination at least for $T=11$ K. The relatively strong thermal quenching of the PL intensity is a formidable barrier to make the same assignment at high temperatures.

We finally show in Fig. 9 the schematic energy-band diagram and PL transitions observed in $CdGa_2Te_4$ for $T=11$ K. The conduction-band and valence-band density of states can be represented by the well-known expressions of $N_C \propto (E-E_C)^{1/2}$ and $N_V \propto (E_V-E)^{1/2}$, respectively. The exponentially tailed donor states of Eq. (7) and broadened Gaussian-like acceptor states of Eq. (8) are also shown in Fig. 9. The acceptor levels determined here are centered at 50 meV (DA1) and 86 meV (DA2) above the top of the valence band, respectively. The double-exponential quenching behavior of the I_{DA1} emission suggests the presence of another impurity or trap level with an activation of $E_X = 9$ meV.

The PL emission caused by transitions from the exponentially tailed or Gaussian-like donor states to acceptor levels showed the typical DA-pair recombination characteristics, as demonstrated in Fig. 8. It is easy to consider that in the vacancy tetrahedral semiconductors such as $CdGa_2Te_4$, the vacancies in the cation sublattice are the origin of the exponentially tailed donor states and Gaussian-like acceptor levels.[14] The photogenerated electrons in the conduction band can be efficiently transferred, via energy relaxation, to the exponential-donor states. The exponential-donor-related emission DA1 is, thus, the dominant PL mechanism in $CdGa_2Te_4$. Reflecting the exponentially tailed donor states, the DA1 emission band observed is strongly asymmetric with tail at the low photon-energy side. An intermixing of the exponential and Gaussian donor states ($E_{D2} = 190$ meV) may be the main cause of the large temperature change in E_p (DA1) and its intensity for $T \geqslant 50$ K (Figs. 5 and 6). The band-to-band emission has never been observed in $CdGa_2Te_4$. This is because always $E_d < E_g$ in $CdGa_2Te_4$. In $ZnIn_2Te_4$, $E_d \leqslant E_g$ for $T \leqslant 90$ K and $E_d > E_g$ for $T > 90$ K; then, the band-to-band emission was observed only for $T > 90$ K.[22]

IV. CONCLUSIONS

We have measured the optical-absorption and PL emission spectra on the defect-chalcopyrite-type ternary semicon-

ductor $CdGa_2Te_4$ in the 0.9–1.5-eV photon-energy range at $T=11-300$ K. The lowest-direct-gap energy E_g of $CdGa_2Te_4$ obtained at 11 K and room temperature are ~1.44 and ~1.35 eV, respectively. The temperature dependence of E_g has been fit using two individual models. The PL spectra have been shown to originate from transitions between the exponentially tailed or Gaussian-like donor states and acceptor levels. The demarcation level width of $E_d=1.417$ eV, a deep donor state located at 190 meV below the bottom of the conduction band, and acceptor levels at 50 and 86 meV above the top of the valence band have also been determined.

[1]A. N. Georgobiani, S. I. Radautsan, and I. M. Tiginyanu, Fiz. Tekh. Poluprovodn. (S.-Peterburg) **19**, 193 (1985) [Sov. Phys. Semicond. **19**, 121 (1985)].
[2]H. Hahn, G. Frank, W. Klingler, A. D. Störger, and G. Störger, Z. Anorg. Allg. Chem. **279**, 241 (1955).
[3]S. Ozaki and S. Adachi, Phys. Rev. B **64**, 085208 (2001).
[4]O. Madelung, in *Landolt—Börnstein: Numerical Data and Functional Relationships in Science and Technology*, edited by O. Madelung (Springer, Berlin, 1985), Vol. 17h.
[5]A. B. Paulavichyus, V. V. Yasutis, Yu. A. Paukshte, and I. P. Burneika, Litov. Fiz. Sb. **17**, 787 (1977).
[6]P. M. Nikolić and S. M. Stojilković, J. Phys. C **14**, L551 (1981).
[7]S. Ozaki, K. Muto, and S. Adachi, J. Phys. Chem. Solids **64**, 1935 (2003).
[8]Y. P. Varshni, Physica (Amsterdam) **34**, 149 (1967).
[9]R. Pässler, Phys. Status Solidi B **200**, 155 (1997).
[10]R. Pässler, Phys. Status Solidi B **216**, 975 (1999).
[11]M. Guzzi and E. Grilli, Mater. Chem. Phys. **11**, 295 (1984).
[12]S. Adachi, in *Handbook on Physical Properties of Semiconductors*, II-VI Compound Semiconductors Vol. 3 (Kluwer, Boston, 2004).
[13]E. Grilli, M. Guzzi, E. Camerlenghi, and F. Pio, Phys. Status Solidi A **90**, 691 (1985).
[14]A. Anedda, L. Garbato, F. Raga, and A. Serpi, Phys. Status Solidi A **50**, 643 (1978).
[15]P. Manca, F. Raga, and A. Spiga, Nuovo Cimento **19B**, 15 (1974).
[16]M. R. Correia, S. Pereira, A. Cavaco, E. Pereira, and E. Alves, Appl. Phys. Lett. **80**, 4504 (2002).
[17]G. B. Abdullaev, V. G. Agaev, V. B. Antonov, R. Kh. Nai, and É. Yu. Salaev, Fiz. Tekh. Poluprovodn. (S.-Peterburg) **6**, 1729 (1972) [Sov. Phys. Semicond. **6**, 1492 (1973)].
[18]G. Couturier, B. Jean, and J. Salardenne, J. Appl. Phys. **78**, 5654 (1995).
[19]E. Grilli, M. Guzzi, P. Cappelletti, and A. V. Moskalonov, Phys. Status Solidi A **59**, 755 (1980).
[20]S. Charbonneau, E. Fortin, and J. Beauvais, Can. J. Phys. **65**, 204 (1987).
[21]S. I. Radautsan, I. M. Tiginyanu, V. N. Fulga, and Yu. O. Derid, Phys. Status Solidi A **114**, 259 (1989).
[22]S. Ozaki, S. Boku, and S. Adachi, Phys. Rev. B **68**, 235201 (2003).
[23]See, for example, D. Curie and J. S. Prener, in *Physics and Chemistry of II-VI Compounds*, edited by M. Aven and J. S. Prener (North-Holland, Amsterdam, 1967), p. 433.
[24]N. M. Gasanly, A. Serpengüzel, A. Aydinli, O. Gürlü, and I. Yilmaz, J. Appl. Phys. **85**, 3198 (1999).